The Computation of Linear Dispersive Electromagnetic Waves

PETER G. PETROPOULOS
Department of Mathematics
Southern Methodist University, Dallas, TX 75275
peterp@ouzo.math.smu.edu

Abstract

Numerical solutions of the equations describing electromagnetic pulse propagation in geometrically complex Debye-dispersive dielectrics are used in the development of safety standards for human exposure to non-ionizing radiation. Debye dispersion is a relaxation process, a phenomenon which occurs when the underlying material is forced into non-equilibrium due to the passing waves. This relaxation is typically stiff in applications, and the system of equations is then singularly perturbed. Such systems are notoriously expensive to solve with standard numerical methods. We review previous work related to the numerical solution of such problems, and consider a representative numerical scheme in order to elucidate the nature of the challenge posed to Computational Electromagnetics by the stiffness. Further, an analysis of the stiffness leads us to propose a scheme that seems "natural" for the problem at hand.

1. Introduction

The development of ultra-short, high-amplitude pulse emitters [1] has put in the spotlight the fact that the electromagnetic properties of real media depend strongly on frequency, i.e., real media are dispersive [2]. The most natural means for studying the interaction of such pulses with complex media is through the numerical solution of the time-domain Maxwell's equations coupled to equations that describe the evolution of the induced macroscopic polarization. These numerical simulations are often used in the assessment of human exposure to high-power pulsed electromagnetic fields during the health and safety analysis of systems involving these pulses. For this reason we are interested in developing prediction tools that are robust and accurate.

The Computational Electromagnetics community has demonstrated a variety of extensions of the popular FD-TD scheme [3] to the modeling of pulse propagation in temporally dispersive media with complex geometry. A representative list of these extensions is [4]-[7]. Some of these approaches append to Maxwell's equations a set of ordinary differential equations, that either describe the local in time constitutive relation [4] involving the displacement $\vec{D}$ and the electric field $\vec{E}$, or the dynamic evolution of the polarization $\vec{P}$ excited by the propagating electric field [5]-[6]. Other approaches use a convolution representation of the constitutive relation which is updated in sync with the time update of the FD-TD discretized Maxwell's equations [7].

The previously published extensions of the FD-TD method to simulate pulse propagation in dispersive dielectrics did not provide any analysis of the accuracy and stability properties of the resultant algorithms, neither was any guidance given for choosing the discretization parameters for a particular medium. Recently, stability and phase error studies were performed for the methods in [4]-[7]. The works [8]-[10] analyzed the spurious numerical properties of the extensions of FD-TD to dispersive dielectrics, and provided guidelines for choosing the discretization parameters so that minimal numerical artifacts would occur. The main conclusions that can be drawn from, e.g., [8] is that **a)** the

timestep must be a small fraction of the shortest relaxation time of the underlying material, and **b)** the Courant number ν [11] must be set with respect to the maximum phase speed in the problem ($\nu = v^{phase}(\omega = \infty)\Delta t/\Delta z$ where $v^{phase}(\omega)$ is the phase speed), and should be chosen as close as possible to the value corresponding to the stability limit of the standard FD-TD ($\nu \leq 1/\sqrt{d}$ where d is the number of spatial dimensions). The algorithms are useful in long-time integrations of the equations when these two conditions are met since then the phase and amplitude errors are minimal for a given medium. Herein, we show how these requirements pose a challenge to the methods in [4]-[7] which severely limits their applicability in realistic cases of scattering of experimentally available pulses from three-dimensional dispersive scatterers.

We now outline the remainder of the paper. Section 2 describes the model equations which we use to develop our analysis in dispersive dielectrics. In Section 3 we present a numerical method, which is an extension of the one in [5], for solving the model equations, and through a dispersion analysis we determine several non-dimensional parameters whose value affects algorithm performance. We also discuss the stiffness issue and the concomitant discretization requirements of the scheme. A reformulation of the model equations in Section 4 allows us to relate the non-dimensional parameters of Section 3 to quantities uniquely pertaining to propagation in dispersive dielectrics and to determine the propagation of high/low frequencies in Debye dielectrics via a singular perturbation analysis [12] of the problem. We close in Section 5 with a discussion of the shortfalls of standard schemes in light of the results presented in Sections 3 and 4, and propose a scheme that is more "natural" for dispersive problems.

2. The Model Problem

In this paper we will be concerned with media whose dispersion is due to relaxation processes. The modeler fits experimentally obtained dielectric data to the complex *relative* permittivity function

$$\epsilon(\omega) = \epsilon_\infty + \sum_{n=1}^{M} \frac{\epsilon_s^n - \epsilon_\infty}{1 - i\omega\tau_n}, \qquad (2.1)$$

for the relevant range of frequencies ω in order to study the propagation of a given electromagnetic pulse in a given material. In (2.1) ϵ_∞ is the infinite-frequency relative permittivity, ϵ_s^n the zero-frequency relative permittivity of the n-th relaxation, and τ_n the n-th relaxation timescale. The fit parameters are ordered so that $\tau_1 > ... > \tau_M$ and $\epsilon_s^1 > ... > \epsilon_s^M$. The phase velocity of harmonic waves in the dielectric is $v^{phase}(\omega) = c/Re\{\sqrt{\epsilon(\omega)}\}$, with c being the speed of light in vacuum. This in turn forces the choice $\epsilon_\infty < \epsilon_s^M$. The parameters for which (2.1) fits water data in the microwave frequency range with $M = 1$ are $\epsilon_s = 80.35$, $\epsilon_\infty = 1.0$, $\tau = 8.13\ ps$. The $M = 1$ water model will be considered later in order to concisely demonstrate the analysis. A typical example of (2.1) for a muscle/fat model is given in [13] where $M = 5$, $\epsilon_\infty = 4.3$, $\epsilon_s^1 = 8 \times 10^5$, $\epsilon_s^2 = 8.19 \times 10^4$, $\epsilon_s^3 = 1.19 \times 10^4$, $\epsilon_s^4 = 36.3$, $\epsilon_s^5 = 51$ and $\tau_1 = 2.31\ ms$, $\tau_2 = 3.7\ \mu s$, $\tau_3 = 238\ ns$, $\tau_4 = 692\ ps$, and $\tau_5 = 8\ ps$. An alternative, ultra-wideband model for water (not used herein) combines Debye and Lorentz media to fit available permittivity data [14].

Using the inverse Fourier transform with (2.1) in the electromagnetic frequency-domain constitutive relation, $\vec{D} = \epsilon_o\epsilon(\omega)\vec{E} = \epsilon_o(\epsilon_\infty\vec{E} + \sum_{n=1}^{M}\vec{P}^n)$, we close the system of Maxwell's equations in the time-domain with M differential equations, one for each Debye relaxation $\vec{P}^n$ ($n = 1, ..., M$) forced by the electric field. For our model problem we will consider a plane pulse normally incident on a homogeneous dispersive half-space from the air side ($z < 0$). The dielectric occupies the half-space $z \geq 0$. The relevant one-dimensional equations are

$$\mu_o \frac{\partial H}{\partial t} = \frac{\partial E}{\partial z},$$

$$\epsilon_o\epsilon_\infty \frac{\partial E}{\partial t} = \frac{\partial H}{\partial z} - \epsilon_o \sum_{n=1}^{M} \frac{\partial P^n}{\partial t}, \qquad (2.2)$$
$$\frac{\partial P^n}{\partial t} = \frac{1}{\tau_n}(\epsilon_o \delta\epsilon^n E_y - P^n); \quad n = 1, ..., M,$$

where ϵ_o and μ_o are respectively the permittivity and permeability of the vacuum, and $\delta\epsilon^n = \epsilon_s^n - \epsilon_\infty$. Apart from ϵ_o and μ_o, all other parameters in (2.2) are obtained by fitting (2.1) to experimental data for the material of interest. In (2.2) the polarization also depends on the spatial coordinate because it is induced by the electric field. The incident electric field is an arbitrary pulse $E^{inc}(z,t) = f(t - z/c)$ of duration T_p. We assume that the half-space is quiescent for $t \leq 0$. Operational considerations fix the incident pulse shape f, and T_p. On the interface, $z = 0$, the total electric field is given by $E(0,t) = f(t) + E^{ref}(0,t) = g(t)$, where E^{ref} is the reflected field. Thus g is known, either by direct measurement of E on the interface, or by measurement of E^{ref} in the air region $z < 0$. This allows us to consider (2.2) in Section 4 as a boundary value problem with zero initial data in the quarter-plane $z \geq 0$, $t \geq 0$, i.e., as a signaling problem.

3. A Numerical Method for the Model Problem

A numerical scheme for (2.2) is

$$\begin{aligned} H_{j+\frac{1}{2}}^{k+\frac{1}{2}} &= H_{j+\frac{1}{2}}^{k-\frac{1}{2}} + \frac{\Delta t}{\mu_o \Delta z}(E_{j+1}^k - E_j^k), \\ E_j^{k+1} &+ \frac{1}{\epsilon_\infty}\sum_{n=1}^{M} P_j^{n,k+1} = E_j^k + \frac{1}{\epsilon_\infty}\sum_{n=1}^{M} P_j^{n,k} \\ &+ \frac{\Delta t}{\epsilon_o\epsilon_\infty \Delta z}(H_{j+\frac{1}{2}}^{k+\frac{1}{2}} - H_{j-\frac{1}{2}}^{k+\frac{1}{2}}), \qquad (3.1) \\ &- \epsilon_o \delta\epsilon^n \frac{\Delta t}{2\tau_n} E_j^{k+1} + (1 + \frac{\Delta t}{2\tau_n}) P_j^{n,k+1} \\ &= \epsilon_o \delta\epsilon^n \frac{\Delta t}{2\tau_n} E_j^k + (1 - \frac{\Delta t}{2\tau_n}) P_j^{n,k}, \end{aligned}$$

where $n = 1, ..., M$ is the relaxation mechanism index, k is the discrete time index, j is the discrete spatial index, and Δt and Δz are respectively the time and spatial steps. Since the polarization is induced by the electric field it is required that these two quantities be collocated in time and space. The reader is referred to [5] for the $M = 1$ version of (3.1).

The scheme (3.1) treats the electric and polarization fields implicitly with the trapezoidal method, and the electric and magnetic fields explicitly with the FD-TD method. Thus, its stability only depends on the Courant number, $\nu_\infty = \frac{c_\infty \Delta t}{\Delta z}$, where $c_\infty = c/\sqrt{\epsilon_\infty}$ is the infinite-frequency phase speed (i.e., the largest speed in the problem). The Courant stability limit is $\nu_\infty \leq 1$ since (3.1) is second-order accurate both in time and space. Common among schemes of equal accuracy in space and time is the consequence that the phase error will be the lowest if ν_∞ is as close to the stability limit ($\nu_\infty \to 1/\sqrt{d}$) as possible. We will see in Section 5 that this is undesirable for dispersive problems. The $M = 1$ case, along with several other schemes for Debye and Lorentz dielectrics, has been investigated in [8]-[10]. For $M > 1$ the numerical dispersion relation from (3.1) is

$$\nu_\infty^2 \sin^2 \frac{\tilde{k}(\omega)\Delta z}{2} = \sin^2 \frac{\omega \Delta t}{2} \times$$
$$(1 + \sum_{n=1}^{M} \frac{v_n - 1}{1 - i \tan \frac{\omega \Delta t}{2} \frac{1}{h_n}}), \qquad (3.2)$$

where $\tilde{k}(\omega)$ is the numerical wavenumber, ω is the real frequency, $v_n = \epsilon_s^n/\epsilon_\infty$, and $h_n = \Delta t/2\tau_n$. The non-dimensional v_n can be interpreted as squares of ratios of phase speed, with v_M being the square of the ratio of the infinite-frequency phase speed over the zero-frequency phase speed (see Section 4). The non-dimensional h_n indicate how well the chosen timestep samples the n-th relaxation timescale. For Debye dielectrics it is always $1 < v_1 < v_2 < ... < v_M$ and, for a fixed timestep, $h_1 < h_2 < ... < h_M$. The numerical dispersion relation (3.2) is compared to the analytical one, $k^2(\omega) = \omega^2 \mu_o \epsilon_o \epsilon(\omega)$ where $\epsilon(\omega)$ is given by (2.1), for a given dispersive medium and the discretization parameters are chosen so that the

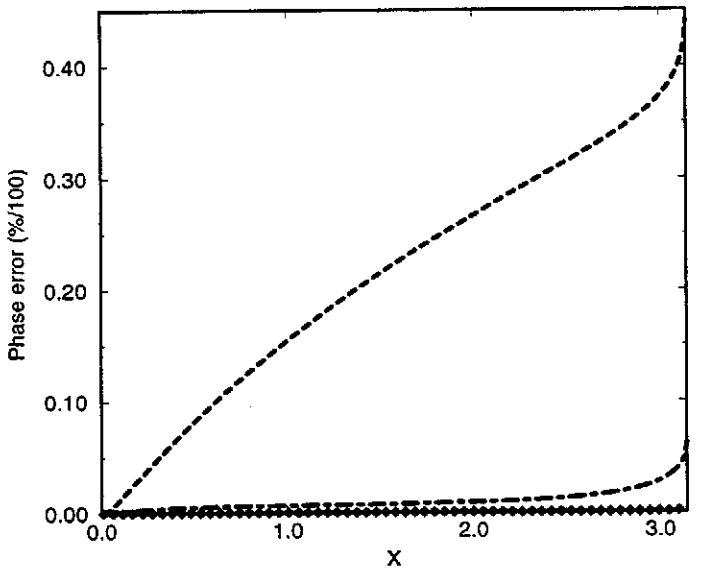

Figure 1: Phase error of the obvious numerical scheme in a medium with $M = 2$ and $\nu_\infty = 1$ for $h_1 = 10^{-4}$, $h_2 = 10^{-1}$ (dashed line), $h_1 = 10^{-5}$, $h_2 = 10^{-2}$ (dash-dot line), $h_1 = 10^{-6}$, $h_2 = 10^{-3}$ (diamond symbols). The horizontal coordinate is $X = \omega\Delta t$.

two dispersion relations agree within a preset accuracy over a desired band of frequencies.

It became obvious in [8] that the parameter $h = \Delta t/2\tau$ has to be $O(10^{-3})$ at least in order to obtain good results in long-time simulations for an $M = 1$ medium. Working with (3.2) one can show that this restriction now applies to h_M. In Figure 1 we demonstrate this for a fictitious (but very reasonable) case of a medium with $M = 2$, $\tau_1 = 8\ ns$, $\tau_2 = 8\ ps$, $\epsilon_\infty = 1$, $\epsilon_s^1 = 80$, and $\epsilon_s^2/\epsilon_s^1 = 10^{-1}$. Note from the Figure that the scheme can be used for a long-time simulation as long as $h_2 \sim O(10^{-3})$. As a result, in a simulation of propagation of a pulse with duration T_p (which, for real sources, is typically $O(10^{-9})$ sec or longer) one can not avoid having to finely resolve τ_M. The $h_M \sim O(10^{-3})$ requirement results in a very small timestep, which then over-resolves the timescale T_p, and, through the Courant condition, in an extremely small spatial step. Realistic problems, e.g., those involving human-sized scatterers composed of such a medium, will quickly grow out of reach of ordinary computational resources. For the muscle/fat model of [13] $\tau_M/\tau_1 \sim 10^{-9}$, and $T_p/\tau_M > 10^3$ for a pulse with $T_p > 10^{-9}$ sec, so we expect the time/spatial steps to be unnecessarily small in this case too. Similarly, for the $M = 1$ water model it is typical that $T_p/\tau > 10^3$ when realistic cases are simulated and again excessive computer resources will be needed.

It is evident that we need numerical schemes that can simulate pulse evolution on timescales which are 2-3 orders of magnitude longer than the smallest relaxation times that arise in applications without having to resolve those small relaxation timescales. Such schemes should be able to maintain their theoretical accuracy for $h_M \gg 1$ when $T_p \gg \tau_M$. A research program in that direction starts with an analysis of (2.2) in order to understand those qualitative aspects of the problem that are unique to dispersive dielectrics and to the presence of stiffness.

4. Analysis of the Model Problem

We determined elsewhere that the more general form of (2.2) for oblique incidence on a dispersive half-space can be reduced to a single partial differential equation (p.d.e.) for the electric field component in the quarter-plane $z \geq 0,\ t \geq 0$. In [15] we derived and analyzed the following signaling problem:

$$\begin{aligned}
&\sum_{l=0}^{M} \beta_l \partial_t^{M-l}(\partial_{tt} - c_l^2 \partial_{zz})E = 0; \quad z > 0,\ t > 0,\\
&E(0,t) = g(t); \quad t \geq 0,\\
&E(z,0) = \partial_t E(z,0) = \ldots = \\
&\partial_t^{M+1} E(z,0) = 0; \quad z \geq 0,\\
&E(z \to \infty, t) \to 0.
\end{aligned} \tag{4.1}$$

Equation (4.1) is a strictly hyperbolic p.d.e. since the $l = 0$ term, which is the principal part of the operator acting on E, has a complete set of $M + 2$ distinct eigenvectors, one for each of

the two distinct eigenvalues $\pm c_0$, and M eigenvectors for the zero eigenvalue of multiplicity M due to the ∂_t^M operating on the $l = 0$ term (see [16] for definition of hyperbolicity). Note that (4.1) also holds in two- and three-dimensions for every component of the electric field if ∂_{zz} is replaced by ∇^2, the appropriate higher dimensional Laplacian. This is because the incident electric field induces the macroscopic polarization so that $\vec{\nabla} \cdot \vec{D} = 0$ implies $\vec{\nabla} \cdot \vec{P} = 0$ everywhere inside a homogeneous medium. Equation (4.1) is also valid for material parameters that are continuously or discretely layered in the z-direction (depth) but invariant with respect to translation in the transverse (x, y) coordinates. The β_l and c_l are given in [15] and form the ordered sequences (in (4.1) $c_0 = c_\infty$)

$$\beta_0 = 1 < \beta_1 < ... < \beta_l < ... < \beta_{M-1} < \beta_M,$$

$$c_0 = v^{phase}(\omega = \infty) > c_1 > \qquad (4.2)$$

$$... > c_l > ... > c_{M-1} > c_M = v^{phase}(\omega = 0).$$

In Debye dielectrics there are $M + 1$ wave families. Each family is described by the appropriate term of the sum in (4.1) while the other terms contribute to its dispersion and diffusion as it propagates. For numerical applications, the most important waves are those that are mainly described by the $l = 0$ and $l = M$ terms in (4.1) as the $l = 0$ term describes the propagation during the time when the pulse first starts interacting with the dielectric, while the $l = M$ term describes the long-time effect of the dispersion on the propagating pulse. This is the reason for studying the $M = 1$ case below.

We proceed with the $M = 1$ water model (see Section 1) in order to demonstrate the techniques involved in analyzing (4.1). The p.d.e. for the electric field now is

$$(E_{ttt} - c_\infty^2 E_{tzz}) + \frac{\epsilon_s}{\epsilon_\infty \tau}(E_{tt} - c_1^2 E_{zz}) = 0, \quad (4.3)$$

where $c_1 = c/\sqrt{\epsilon_s}$ is the zero-frequency phase speed, and $\frac{\epsilon_s}{\epsilon_\infty \tau} \sim O(10^{13})$ sec^{-1}. To determine how the high frequencies (short-time behavior) propagate in Debye media we substitute $E(z,t) = u(z,t)H[\phi(z,t)]$ in (4.3), where the Heavyside function is $H[\phi] = 0$ (1) for $\phi \geq 0$ ($<$ 0), and $u(z,t)$ represents the smooth part of the solution. With this substitution we determine the wavefront surface, $\phi(z,t)$, and the behavior of $u(z,t)$ on the wavefront. We find that $\phi(z,t) = z \pm c_\infty t$, i.e., that the characteristics are straight lines and have speed c_∞, and determine that on the wavefront, $\phi(z,t) = z - c_\infty t = 0$, $u(z,t)$ satisfies

$$u_t + c_\infty u_z + \frac{\epsilon_s}{2\epsilon_\infty \tau}(1 - \frac{c_1^2}{c_\infty^2})u = 0. \qquad (4.4)$$

The solution of this p.d.e. shows that the high-frequency components of the electric field decay exponentially fast in a spatial interval of length $c_\infty \tau$ ($\sim O(10^{-3})$ m for water) which we have previously labeled the "time-domain skin-depth" [15]. Thus, our problem has a small spatial scale due to the time stiffness since (4.4) is hyperbolic. In this short depth, the low frequencies will only be advected with speed c_∞ as the material has not had time to react. The procedure just outlined can also be though of as a short-time asymptotic analysis of the problem. In addition, it indicates that any discontinuities in the signaling data will propagate on the characteristics of (4.3) and their amplitude will decay exponentially.

Next we consider (4.3) taking into account the largeness of $\frac{\epsilon_s}{\epsilon_\infty \tau}$. We define the small parameter $\epsilon = \frac{\epsilon_\infty \tau}{\epsilon_s}$, and note that ϵ/T_p is still very small ($\leq O(10^{-4})$) for nanosecond (or longer) pulse duration. The assumptions which make the analysis possible are reasonable in light of experimental reality. Here is our singularly perturbed problem statement:

$$\epsilon\,(E_{ttt} - c_\infty^2 E_{tzz}) +$$

$$(E_{tt} - c_1^2 E_{zz}) = 0; \quad z > 0,\ t > 0,$$

$$E(0,t) = g(t); \quad t \geq 0, \qquad (4.5)$$

$$E(z,0) = \partial_t E(z,0) = \partial_{tt} E(z,0) = 0; \quad z \geq 0,$$

$$E(z \to \infty, t) \to 0,$$

where $g(t)$ is defined in Section 2. To analyze (4.5) as $\epsilon \to 0$ we expand the solution in powers of the small parameter, i.e., $E(z,t) = E^0(z,t)+\epsilon E^1(z,t)+...$, and find that the zeroth-order term satisfies $E^0_{tt}-c_1^2 E^0_{zz} = 0$. The solution of this "outer" problem is

$$\begin{aligned} E^0(z,t) &= g(t-z/c_1); \quad z \le c_1 t \\ &= 0; \quad z > c_1 t. \end{aligned} \tag{4.6}$$

We see that the discontinuity, generated at $t = 0$ due to the turn-on of $g(t)$, will propagate along the sub-characteristics of speed c_1 instead of propagating along the true characteristics of (4. 3) which we found in the previous paragraph.

To resolve this inconsistency we introduce an internal boundary-layer on the sub-characteristic $z = c_1 t$ through a space-like limit process

$$\begin{aligned} x^* &= \frac{z-c_1 t}{\delta(\epsilon)}; \quad \delta(\epsilon) \to 0 \\ t^* &= t \end{aligned} \tag{4.7}$$

and an "inner" expansion

$$E(z,t;\epsilon) = E^0(x^*,t^*) + \mu(\epsilon)E^1(x^*,t^*) + ..., \tag{4.8}$$

where $\mu(\epsilon)$ is an order parameter that depends on ϵ in general. We change to the "inner" variables (x^*,t^*) in (4.5) and substitute the "inner" expansion in the resulting p.d.e. We display below the most important terms to zeroth-order in $\mu(\epsilon)$ since we will have to match the first term of the "inner" expansion to the solution (4.6) of the "outer" problem (which is of zeroth-order in ϵ) to determine $\delta(\epsilon)$:

$$\begin{aligned} &\frac{\epsilon}{\delta^2(\epsilon)}[-c_1^3 E^0_{x^*x^*x^*} + c_1 c_\infty^2 E^0_{x^*x^*x^*} + ...] \\ &= 2c_1 E^0_{x^*t^*} + ... \end{aligned} \tag{4.9}$$

In order for the terms displayed in (4.9) to balance we have to choose $\delta(\epsilon) = \epsilon^{1/2}$. Integrating out one of the ∂_{x^*} we obtain a heat equation, i.e., $E^0_{t^*} = \frac{c_\infty^2 - c_1^2}{2} E^0_{x^*x^*}$, for the field on and near (within a space-like interval of width $\epsilon^{1/2}$) the sub-characteristic of speed c_1. This heat equation describes the part of the incident pulse which propagates deep in the medium (past the "skin-depth"). To see that propagation (albeit at a much slower speed) is maintained even though the problem now has a strong parabolic character we use the inverse of the coordinate change in (4.7) to produce the advection-diffusion equation of [15]:

$$E^0_t + c_1 E^0_z = \frac{\epsilon_\infty \tau}{2\epsilon_s}(c_\infty^2 - c_1^2)E^0_{zz}. \tag{4.10}$$

The derivation of the uniformly valid perturbation expansion of the solution, along with the the analogous procedure for Lorentz dielectrics, will be presented elsewhere.

The method of analysis in this Section differs from that used in [15]. However, the obtained analytical results validate each other, and the method used here lends itself to application to *difference equations* with the purpose of determining scheme behavior in the presence of stiffness.

5. Discussion

We know that the timestep, Δt, of second-order accurate Leapfrog-based schemes (FD-TD) for dispersive electromagnetic problems must finely resolve the shortest relaxation timescale τ_M in order to achieve reasonable accuracy over long-time simulations of pulse propagation. In Section 3 we indicated how this requirement, coupled with the requirement on ν, results in a need for large amounts of computational resources. It is tempting to accept the small timestep at the expense of linearly increasing the run time and lower the Courant number (effectively increase the spatial step keeping the timestep fixed) in order to save on core memory by using fewer spatial cells. However, the standard schemes are then faced with a challenge as they do not allow a reduction of ν; the algorithms in [4]-[7] become more dispersive as ν is reduced. Thus, it is reasonable to look for schemes whose performance does not

degrade as the Courant number is lowered below the maximum value required for stability. Further, in Section 4 we determined that the pulse response in a relaxing dielectric is mainly a diffusion wave traveling with the zero-frequency phase velocity of harmonic waves. We also found that the fastest speed, i.e., the infinite-frequency phase velocity, is important only in a thin layer near the air/dielectric interface in which the response is hyperbolic and decays exponentially. The stiffness due to the large magnitude of the β_M in (4.1) (or $\epsilon_s/\epsilon_\infty\tau$ in (4.3)) resulted in the fast speed being important only in a short time interval of $O(\tau)$ sec after the pulse has started interacting with the dispersive dielectric. As an example, in the $M = 1$ model of water permittivity this thin interval corresponds to a depth of $O(10^{-3})$ m, and thus the slow speed $c_1 \sim c_\infty/9$ is the dominant speed in the model. It must be emphasized that in the system (2.2) the speeds c_l, $1 \leq l \leq M$, were not evident and that only the reformulation enabled us to calculate them (see also [15]). These speeds are disparate for typical experimentally determined permittivity properties.

Next we use the results summarized in the previous paragraph to demonstrate the implications for numerical schemes of the time stiffness and of the disparate wavespeeds in the dispersive dielectric. In a typical one-dimensional computation we would use the results from [8]-[10] to set the timestep and the Courant number ν. Since the Courant number for stability is set with respect to the highest speed in the problem these actions have thus fixed the spatial cell size for the computation to be $\Delta z_0 = c_0\Delta t/\nu$. If now we assume that the remaining M wave types in (4.1)-(4.2) are decoupled, then the spatial step for each type is determined by $\Delta z_n = c_n\Delta t/\nu$, $n = 1, ..., M$, where c_n and Δz_n are respectively the wavespeed and spatial step associated with the n-th wave type. Thus, for a fixed timestep and Courant number, the spatial steps for the most important waves in the problem (the $l = 0$ and $l = M$ waves) are related as (using $c_0 = c_\infty$)

$$\Delta z_M = \frac{c_M}{c_\infty}\Delta z_0. \tag{5.1}$$

Consequently we are using the wrong spatial cell size since $\Delta z_0 > \Delta z_M$. It turns out that in explicit finite difference schemes for hyperbolic problems with multiple wave speeds the stability requirement is based on the highest speed in the problem while the spatial resolution is based on the lowest speed. That the slowest wave speed must be used to set the spatial resolution can be understood by the following argument. Consider a fixed frequency f; the wavelength associated with the slow speed is smaller than that associated with the fast speed through the relation $wavespeed = wavelength \times f$. This is because initially the pulse will just decay exponentially in a very short interval and all of its frequency components will travel with the fast speed c_∞ since the material has not had time yet to react dispersively. Thus, a small length scale develops in time because gradually the pulse will slow down and travel with speed c_M. Since the slow speed is responsible for a small length scale we should set our discretization to sample it adequately. The cell size thus determined is Δz_M. We deduce that the disparate speeds then *require* a reduction of the Courant number since using the Δz_M from (5.1) in the stability restriction $c_0\Delta t/\Delta z_M = \nu$ (having set ν and Δt previously) we obtain the effective Courant number for the computation to be $c_0\Delta t/\Delta z_0 = \nu c_M/c_0 = \nu' < \nu$; the effective Courant number ν' is *lower* than the Courant number set so that the standard scheme would introduce as little artificial dispersion as possible. Thus the main response is not well captured. For the materials of interest to bioelectromagnetics it is $0.1 < c_M/c_0 < 0.5$ and thus the standard schemes deteriorate as the propagation evolves. Another way to see this is by referring to Figure 2 where the stencil of the FD-TD method in one dimension is shown. Setting the Courant number to be the maximum allowed by stability considerations ($\nu = 1$ in one dimension) corresponds to using information along the characteristics of the equations which have slope

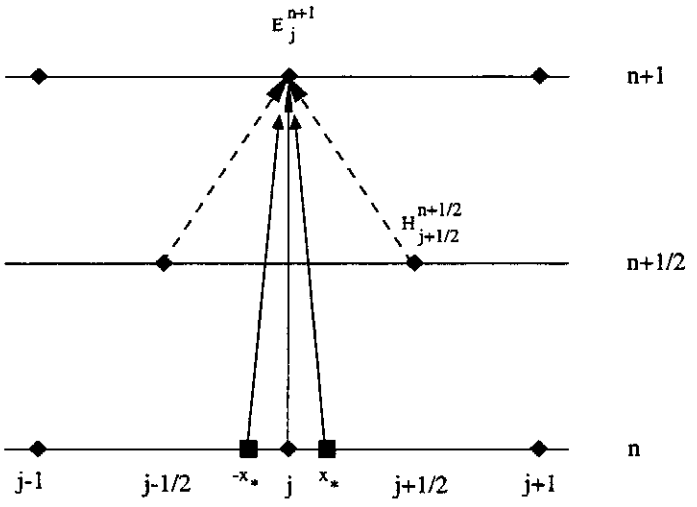

Figure 2: Space-time stencil of the FD-TD scheme.

$1/c_\infty$ and then E_j^{n+1} depends on $E_{j\pm1}^n$, E_j^n, and E_j^{n-1}, as one can show by eliminating the magnetic field from the difference equations. This dependency reflects a fundamental property of the partial differential equation only when information on the grid indeed travels with the characteristic speed but we saw for dispersive dielectrics that the fast characteristic speed c_∞ is important only during a short time interval. Past that time interval the sub-characteristic slow speed, c_M, is important and then field information travels between time levels along the lines of slope $1/c_M$, i.e., electric field information travels along the arrows from time level n to $n+1$ that are attached at $\pm x_*$ in Figure 2. To capture this feature of the propagation one needs to lower the Courant number but standard schemes then become more dispersive. Alternatively, one could redefine the spatial differencing operators in the electric field update of the FD-TD scheme to use magnetic field data at the intersections of the solid lines connecting $E_{\pm x_*}^n$ and E_j^{n+1} with the time level $t = (n+1/2)\Delta t$ in Figure 2. A similar redefinition should then be done to the spatial differencing operators used in the magnetic field update.

In summary, finite difference schemes which are second-order accurate in both time and space, the so called $(2-2)$ schemes (FD-TD among them), require that the Courant number used be the maximum allowed for stability ($\nu = 1$ in one dimension) in order for them to introduce the least phase error. Here we have shown that in the framework of the standard schemes the dominant waves in dispersive problems are then calculated with an effective Courant number which is less than ν and standard schemes then do not preserve a fundamental property of the equations involved. However, $(2-4)$ schemes that are second-order accurate in time and fourth-order accurate in space operate well for $0.1 < \nu < 0.4$, and do not suffer from a phase error degradation as the Courant number is decreased [17]. In addition, these schemes are overall fourth-order accurate for $\Delta t \sim O(1)\Delta z^2$. This is equivalent to reducing the Courant number while keeping the spatial step fixed, or increasing the spatial step while keeping the timestep fixed. Also, this relationship between the time and the spatial steps in the $(2-4)$ scheme is like the diffusion scaling $t \sim O(1)z^2$ which appears in our problem asymptotically due to (4.10). We expect such schemes to maintain their accuracy as the time stiffness parameter h_M becomes larger than one. Numerical validation of this conjecture about the suitability of the high-order methods for dispersive problems is the subject of our current research.

Acknowledgements

This work was supported in part by AFOSR under grant F49620-95-1-0014.

References

[1] See papers on Pulse Generation and Detection in *Proceedings of the Second International Conference on Ultra-Wideband Short-Pulse Electromagnetics*, L. Carin and L. B. Felsen, Eds. New York: Plenum Press (1995).

[2] J. D. Jackson, *Classical Electrodynamics*, 2nd ed. New York: Wiley (1975).

[3] A. Taflove and K.R. Umashankar, "The Finite-Difference Time-Domain (FD-TD Method for Elec-

tromagnetic Scattering and Interaction Problems," *J. Electromag. Wav. Appl.*, vol. 1, no. 3, pp. 243-267, 1987.

[4] R.M. Joseph, S.C. Hagness and A. Taflove, "Direct Time Integration of Maxwell's Equations in Linear Dispersive Media with Absorption for Scattering and Propagation of Femtosecond Electromagnetic Pulses," *Optics Lett.*, vol. 16, no. 18, pp. 1412-1414, 1991.

[5] T. Kashiwa, N. Yoshida and I. Fukai, "A Treatment by the Finite-Difference Time-Domain Method of the Dispersive Characteristics Associated with Orientation Polarization," *IEICE Transactions*, vol. E73, no. 8, pp. 1326-1328, 1990.

[6] T. Kashiwa and I. Fukai, "A Treatment by the FD-TD Method of the Dispersive Characteristics Associated with Electronic Polarization," *Microw. Optic. Tech. Lett.*, vol. 3, no. 6, pp. 203-205, 1990.

[7] R. Luebbers, D. Steich and K. Kunz, "FD-TD Calculation of Scattering from Frequency-Dependent Materials," *IEEE Trans. on Antennas and Propagation*, vol. 41, no. 9, pp. 1249-1257, 1993.

[8] P. G. Petropoulos, "Stability and Phase Error Analysis of FD-TD in Dispersive Dielectrics," *IEEE Trans. on Antennas and Propagation*, vol. 42, no. 1, pp. 62-69, 1994.

[9] C. Hulse and A. Knoesen, "Dispersive Models for the Finite-Difference Time-Domain Method: Design, Analysis, and Implementation," *J. Opt. Soc. Am. A*, vol. 11, no. 6, pp. 1802-1811, 1994.

[10] J. L. Young, A. Kittichartphayak, Y. M. Kwok and D. Sullivan, "On the Dispersion Errors Related to $(FD)^2TD$ Type Schemes," *IEEE Trans. on Microwave Theory and Techniques*, vol. 43, no. 8, pp. 1902-1910, 1995.

[11] J.C. Strikwerda, *Finite Difference Schemes and Partial Differential Equations*, Pacific Grove CA: Wadsworth and Brooks/Cole (1989).

[12] C. M. Bender and S. A. Orszag, *Advanced Mathematical Methods for Scientists and Engineers*, McGraw-Hill, New York (1978).

[13] W. D. Hurt, "Multiterm Debye Dispersion Relations for Permittivity of Muscle," *IEEE Trans. on Biomedical Engineering*, vol. 32, pp. 60-64, 1985.

[14] H. J. Liebe, G. A. Hufford and T. Manabe, "A Model for the Complex Permittivity of Water at Frequencies Below 1 THz," *Int. J. of Infrared and Millimeter Waves*, vol. 12, pp. 659-675, 1991.

[15] P. G. Petropoulos, "The Wave Hierarchy for Propagation in Relaxing Dielectrics," *Wave Motion*, vol. 21, pp. 253-262, 1995.

[16] F. John, *Partial Differential Equations*, Springer-Verlag, New York (1982).

[17] P. G. Petropoulos, "Phase Error Control for FD-TD Methods of Second and Fourth Order Accuracy," *IEEE Trans. on Antennas and Propagation*, vol. 42, no. 6, pp. 859-862, 1994.